RSC Advances

ROYAL SOCIETY OF CHEMISTRY

www.rsc.org/advances

Graphical Abstract

Solvent-Free Click Chemistry for Tetrazole Synthesis from 1,8-diazabicyclo[5.4.0]undec-7-ene (DBU)-Based Fluorinated Ionic Liquids, their Micellization, and Density Functional Theory Studies

Abdul Hameed, Syed Abid Ali, Ali Anus Khan, Syed Tarique Moin, Jamshed Hashim, Khalid Mohammed Khan, Fatima Zahra Basha, Muhammad Imran Malik

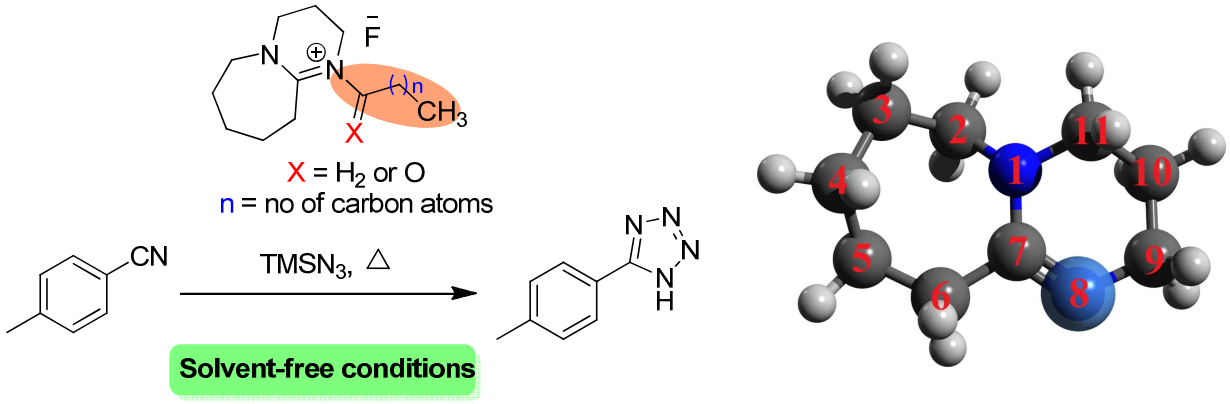

Solvent-Free Click Chemistry for Tetrazole Synthesis from 1,8-diazabicyclo[5.4.0]undec-7-ene (DBU)-Based Fluorinated Ionic Liquids, their Micellization, and Density Functional Theory Studies

Abdul Hameed**, Syed Abid Ali, Ali Anus Khan , Syed Tarique Moin , Khalid Mohammed Khan , Jamshed Hashim , Fatima Zahra Basha , Muhammad Imran Malik*

H. E. J. Research Institute of Chemistry, International Center for Chemical and Biological Sciences, University of Karachi, Karachi-75270, Pakistan

Corresponding authors:

** A.H., Email: abdul.hameed@iccs.edu / abdul_hameed8@hotmail.com

* M.I.M., Email: m.imran.malik1@gmail.com / mimran.malik@iccs.edu

Tel.: +92-219-9261701-2; Fax: +92-213-4819018

Abstract

In the present study, we have synthesized novel 1,8-diazabicyclo[5.4.0]undec-7-ene (DBU)–based fluorinated ILs (DBUF-ILs) simply by solvent-free quaternization and subsequent anion (F-) exchange reactions. The micellization behavior and density functional theory (DFT) calculations of DBUF-ILs have been conducted. The DFT calculations of some selected DBU derivatives show the *N*-substitution effect on DBU geometry. In addition to the geometry analysis of these DBU derivatives, HOMO and LUMO energies, and band gaps were also calculated that give insight into different types of transitions and electronic effects. The stability of the DBU derivatives was also investigated *via* binding energy calculations based on the DFT method. A click chemistry reaction for tetrazole formation is performed under solvent-free thermal and microwave irradiation. Yields obtained were in the range of 70-95%. Complete structural characterization of each product was accomplished by several modern techniques including ^{1}H NMR, ^{13}C NMR, EI^{+} and/or FAB mass spectrometry, IR and UV spectroscopy.

Keywords: 1,8-diazabicyclo[5.4.0]undec-7-ene (DBU), Ionic liquids, Fluoride anion, micellization, Density functional theory calculation, Click chemistry, Tetrazole formation

1. Introduction

The concept of ionic liquids (ILs) has been conceived in early 19th century. After a lull of almost a century, interest in synthesis and applications has evolved again for last couple of decades. [1] Because of excellent physiochemical properties such as low volatility, high thermal stability, along with its great recycling potential; ionic liquids are a decent replacement of traditional toxic solvents for organic synthesis with enhanced eco-friendly conditions. [2, 3] The ILs are usually synthesized by the quaternization of heterocyclic compounds. Inert nature of imidazole based ILs make them widely applicable in organic synthesis. [4-6] In this study, we used DBU (1,8-Diazabicyclo[5.4.0]undec-7-ene) as a head group to synthesize the task specific *N*-alkylated ionic liquids *via* quaternization reaction. The role of DBU as a catalyst or hindered base is well reported. DBU offers excellent selectivity in many organic reactions compared to other organic bases. [7, 8] Removal of DBU from reaction mixture is difficult and tedious, however, DBU based ILs with same basicity would minimize such problems. [9] To the best of our knowledge, *N*-

alkylated or acylated DBU based ILs have never been employed as catalysts or promoters in organic reactions. The salts of acetic and lactic acids prepared *via* neutralization reaction with DBU have been used as solvent and catalysts to preform aza-Micheal addition [4, 10] and carbonylation. [9]

In the present study, we aimed to synthesize DBU based fluorinated ILs (DBUF-ILs) connected to a range of alkyl or acid halides of varying carbon chain lengths *via* quaternization reaction. Corresponding counter ions of the resultant ionic compounds would be exchanged with fluoride due to its better reactivity as a base. [11] In addition, it develops a relationship with TBAF (tetra butyl ammonium fluoride) that has diverse applications in organic synthesis. Although TBAF has versatile applications in organic synthesis, no selectivity (such as deprotonation or dehalogenation etc.) in organic reactions is possible that might be offered by DBU-based ILs. [12] To determine the applicability of synthetic DBUF-ILs in organic synthesis, we initially chose the click chemistry reaction of tetrazole formation. Tetrazole serves as surrogate of carboxylic acid and occupies a unique position in pharmaceutical chemistry because of its capability to improve the metabolic and pharmacokinetic properties of drugs. [13] Additionally, the physiochemical property such as micellization of DBUF-ILs as potential drug carrier has also been carried in water to determine the effects of different parameters such as, temperature, pH, and concentration on the hydrodynamic radius of the micelles. Structural insight of some selected compounds was obtained by density functional theory (DFT) calculations. The stability of DBU based ionic salts was also of great concern, since they may exist in the form of ionic liquids, therefore, binding energies calculations were performed for the selected DBU derivatives in comparison to TBAF.

Tetrazole formation was carried out under solvent-free conditions by using traditional thermal and microwave irradiations. The reaction time and yield of the tetrazole were found to be better under microwave conditions. Cumulatively, the present study describes the synthesis of DBUF-ILs, their micellization behavior, DFT calculations and synthetic application in click chemistry.

2. Results and discussion

2.1. Synthesis of DBUF-ILs (2a-2j)

A general strategy to synthesize the DBU-based ILs was comprised of two steps i.e. 1) the quaternization under solvent-free conditions, and 2) exchange of counter anion with fluoride

anion (Scheme 1). The yields of final DBUF-ILs **2a–2j** with fluoride counter anion were found in the range of 70-95% (Table 1).

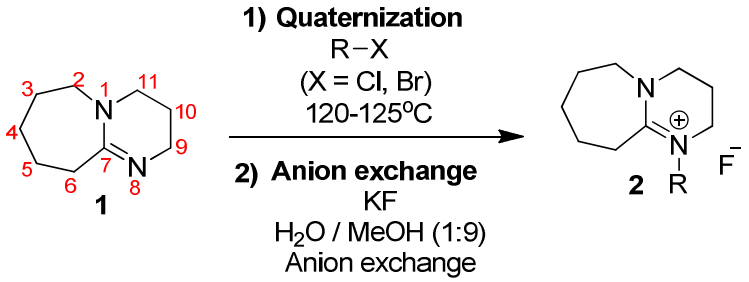

Scheme 1: Synthesis of DBU base ionic liquids **2a-2j**

Table 1: Synthesis of DBU-ILs **2a-2j** *via* Quaternization and halide (F^-) anions exchange

Compounds	R = Alkyl chain	Time (h) Quaternization / Anion Exchange	Yield (%)
2a	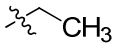	2 / 0.5	95*
2b	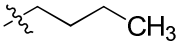	14 / 1	90
2c	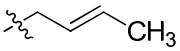	5 / 1	80
2d	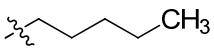	5 / 1	80*
2e	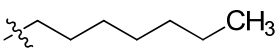	5 / 1	88*
2f	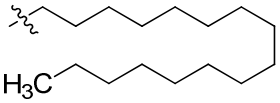	14 / 2	80
	R = Acyl chain		
2g	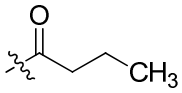	5 / 1.5	76*
2h	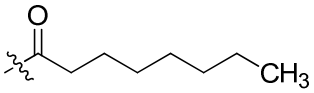	14 / 1.5	83
2i	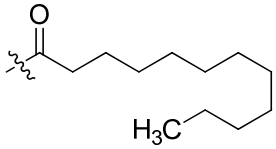	14 / 1.5	74

2j	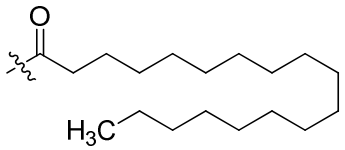	14 / 2	80

* Reactions were scaled up to grams (3-5 g, 20-33 mmol) with DBU as starting material.

The quaternization of DBU was performed under solvent-free conditions with either alkyl halides or acid halides of different chain lengths (C^2 to C^{16}) to obtain corresponding *N*-alkylated or acylated products **2a**–**2j** (Table 1). The study reveals the impact of alkyl chain length in the activity of ILs. In quaternization step, different reaction times for completion of reaction are noticed for alkyl and acid halides because of unlike characteristic of leaving halides ions. The halide substrates with poor leaving group ($Cl^- < Br^-$) or long alkyl chain required longer reaction time compared to others in the series (Table 1). The counter anions either Cl^- or Br^- of each resultant ILs were replaced with fluoride anion. The counter anion exchange reaction was performed with potassium fluoride solution in solvent mixture (Water / Methanol, 1:9 ratio) by shaking the resultant ILs. Thin layer chromatographic analysis was carried at this step to ensure the absence of prior ILs as starting materials. Varied amounts of potassium fluoride (3–7.5 equiv.) were used because of dissimilar leaving abilities of different halides ($Cl^- < Br^-$) along with necessary adjustments in temperature and reaction time. Some reactions were scaled-up to 30 mmol of DBU as starting material to broaden the reaction scope. The structures of all the synthetic DBU derivatives were confirmed by different spectroscopic techniques that include ^{1}H NMR, ^{13}C NMR, EI-MS, IR and UV spectroscopy.

2.2. Micellization Study

The amphiphilic nature and self-association behavior of ionic liquid in aqueous solution makes them fascinating surfactants. [8, 14-22] Imidazolium ionic liquids have been used by most of the researchers with conductivity and surface tension measurements as a tool for determination of critical micelles concentration (cmc) of the ionic liquid in aqueous solution. In a recent paper, Mahajan *et al.* [8] reported three DBU-based ionic liquids with longer alkyl chains (C_{12}, C_{14}, C_{16}) and bromide as counter ions. They determined critical micelles concentration by conductivity and surface tension measurements. Herein, we focused on the shorter alkyl chains and determined the hydrodynamic radius of the formed micelles in aqueous solution by dynamic light scattering (DLS). The hydrodynamic radius of the micelles with 1 wt% of ILs in deionized

water is summarized in Table 2. Most of the products under study formed monomodal micelles. The 1 wt% IL **2e** formed turbid solution and is further diluted to 0.1 wt.% for clear solution. Unlike other products, the micelles formed by DBU derivative **2e** were polydisperse even at lower concentrations. The aim of current study is to evaluate the effects of different variable such concentration, temperature and pH on the stability and size of the micelles. The IL **2c** has been selected for further detailed investigation. As a typical example, the data obtained from DLS is demonstrated in Figure 1. Part A of Figure 1 is the autocorrelation function (ACF) and intensity distribution of the purified liposome as a control. Figure 1B depicts the autocorrelation function of DBU derivative **2c** indicating the intense monomodal signal of the measurement. Figure 1 C-D illustrate 3D and 2D intensity histogram of the sample, the reproducibility and intensity of the signals is clearly demonstrated. As can be seen in Figure 1E, the hydrodynamic radius of 1 wt% solution of DBU derivative **2c** is calculated as 224.4 nm with ~9% error function.

As a next step, stability of formed micelles was studied by varying the parameters of concentration, temperature and pH. Figure 2A demonstrates effect of concentration on the hydrodynamic radius of the micelles and it can be clearly seen that hydrodynamic radius remain fairly constant within the error limits in the concentration range of 0.1 to 7.5 wt%. On the contrary, hydrodynamic radius changed with a clear trend with variations in pH and temperature. Size of the micelles and polydispersity increased as pH of the solution was altered from neutral to acidic or basic (see Figure 2B). The solution of ionic liquid was heated/cooled to desired temperature and kept there for 15 min. After the temperature treatment, samples were cooled down to room temperature prior to DLS measurements. As can be seen in Figure 2B, temperature treatment induced an increase in hydrodynamic radius and polydispersity of the micelles. The size of the micelles increased up to ca. 50˚C and remained fairly constant afterwards with slight rise in the polydispersity of the micelles with further increase in temperature. Nonetheless, the micelles were extremely stable over a wide range of concentration, pH and temperature.

Table 2: Hydrodynamic radius of DBU based ionic liquid as obtained by DLS (1 wt % unless otherwise specified)

Compounds	Hydrodynamic Radius (nm)
2a	157±14%

2b	106±23%
2c	224±9%
2d	186±16%
2e*	345±16%, 374±18%
2g	171±15%

*0.01 wt. %

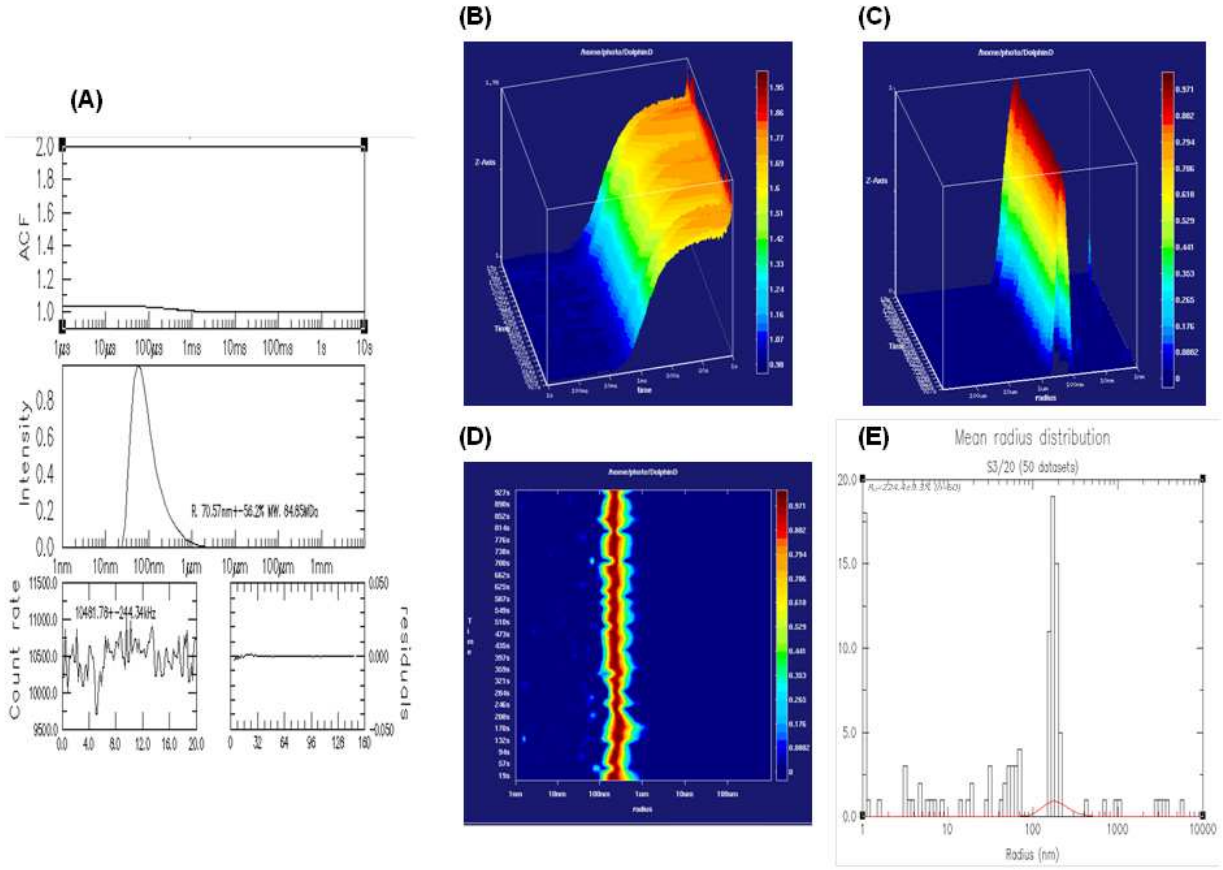

Figure 1: DLS measurement for the hydrodynamic radaii (R_H) of the purified liposome (as standard control) and the 1 wt% micelles of DBU derivaitive **2c** (as a typical example) performed on Laser-spectroscatter 201 (RiNA, Berlin Germany). (A) Autocorrelation function (ACF) and intensity distribution of the purified liposome (in PBS pH7.4). (B) superpose autocorrelation function of test compound 3, (C-E) 3D and 2D Intensity histograms illustrate the cumulated dataset of 50 measurements of liposome (R_H= 70.5 nm) and compound 3 (R_H=224.4 nm ± 9.3), respectively.

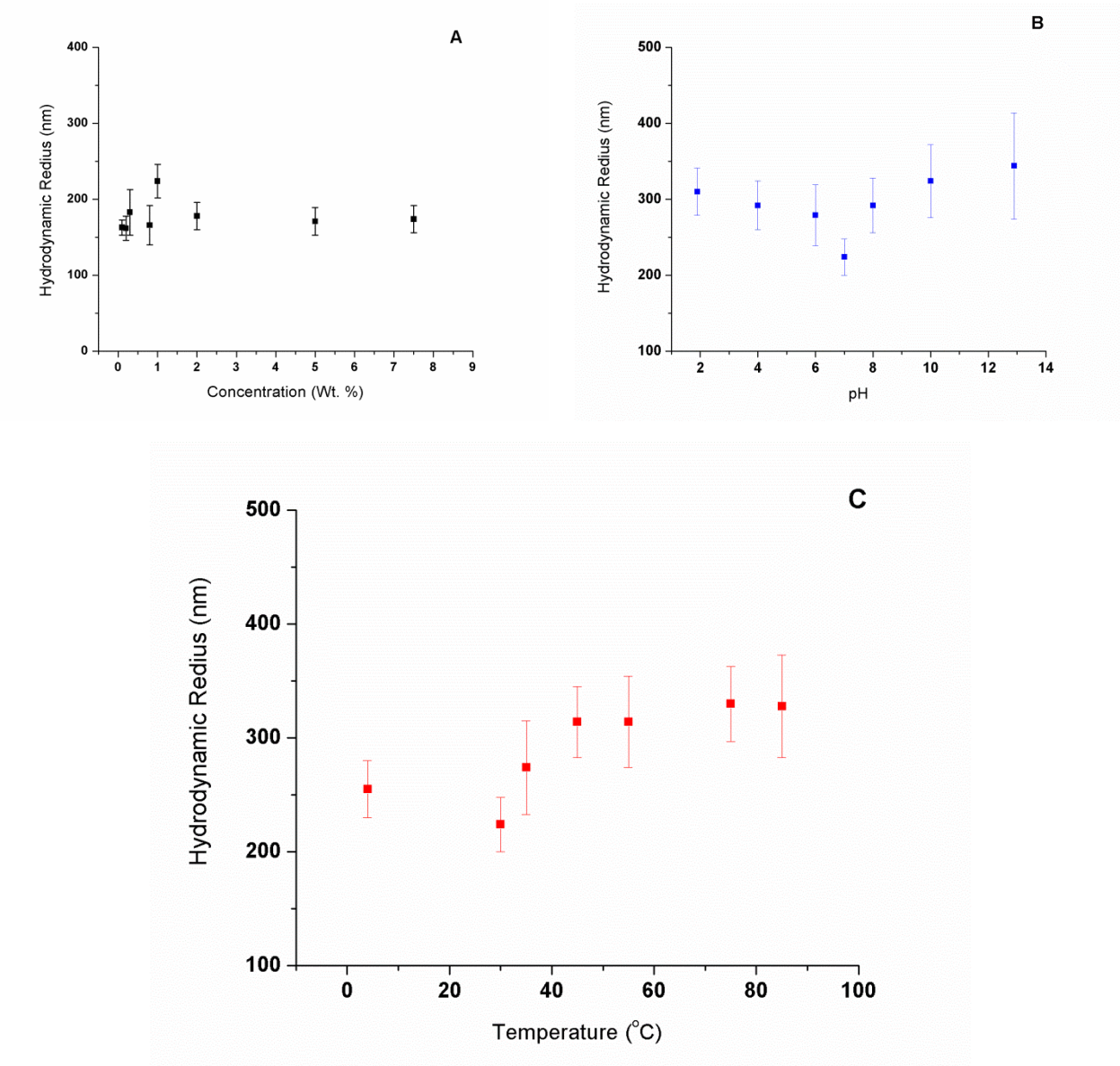

Figure 2: Effect of different variables on the hydrodynamic radius (R_H) of micelles of DBU derivative **2c**, (A) concentration of ionic liquid, (B) pH (concentration 1 wt%), and (C) temperature (concentration 1 wt %).

2.3. Geometrical analysis

The purpose of including the theoretical study here was to gain an insight into the effect of different substituents on the DBU compound. Table 3-4 lists the bond lengths and bond angles of these derivatives including the DBU compound.

DBU compound contains a characteristic C=N bond having the bond length of 1.29 Å, which is an obvious characteristic of the double bond along with other C-C and C-N bonds. During the synthesis of DBU derivatives, the quaternization was likely to occur at the nitrogen atom of the C=N bond thus forming *N*-substituted cationic compounds that exists as salts with corresponding counter ions. The counter ions were replaced with fluoride ion later. The key point was to observe the changes of the configuration of DBU compound after the *N*-substitution. Based on the DFT results, the C=N bond length of these DBU derivatives varies between 1.43 and 1.47 Å that is significantly different from that of DBU compound. As can be seen, the carbonyl substitution (compound **2g**) has remarkably increased the C=N bond length (1.47 Å) in comparison to the alkyl substituted DBU derivatives whose bond length varied between 1.42 to 1.43 Å. Increased C=N bond lengths by 0.13-0.18 Å in *N*-substituted derivatives is attributed to the partial double bond character and delocalization of electrons in these compounds. Increased C=N bond length in case of compound **2g** compared to other investigated derivatives was due to the strong electron withdrawing effect of the carbonyl moiety that is directly attached to the nitrogen atom, thus leading to the elongation of the bond length. In case of alkyl based DBU derivatives, such effect was also observed due to quaternary substitution and consequently increased C=N bond lengths were noticed. However, an increase in the number of carbon atom in the substituent groups makes no difference in the bond lengths. Apart from the C=N bond length elongation that is an indicative of the single bond character, rest of bonds were unperturbed by the *N*-substitution as is evident from the bond length data (cf. Table 3).

In addition to the analysis of bond lengths variation, bond angles were also examined and compared with that of the DBU compound listed in Table 4. Bond angles involving the C=N atoms namely C^5-C^6-C^7, C^6-C^7-N^1, C^6-C^7-N^8, C^7-N^8-C^9, N^1-C^7-C^8, N^8-C^9-C^{10}, C^7-N^1-C^2 and C^{11}-N^1-C^7 were also computed from the optimized structures. It was observed that the substitution at the nitrogen atom caused three bond angles (C^5-C^6-C^7, C^7-N^8-C^9 and N^1-C^7-N^8) to deviate from those in the DBU compound. A similar trend in the variation of bond angles was observed for all substituted compounds. In the case of compound **2g** that has a carbonyl substituent deviates a little more compared to those in the DBU compound. All other bond angles showed a negligible effect due to *N*-substitution of the DBU compound.

Table 3: Calculated bond lengths in Å for the optimized DBU and its selected derivatives.

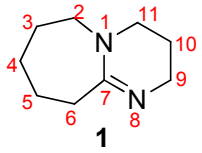

1

Bond Lengths	Compounds					
	DBU	2b	2c	2e	2f	2g
C^2-C^3	1.53	1.54	1.56	1.54	1.54	1.54
C^3-C^4	1.54	1.54	1.54	1.54	1.54	1.53
C^4-C^5	1.54	1.54	1.54	1.54	1.54	1.53
C^5-C^6	1.54	1.54	1.54	1.54	1.54	1.53
C^6-C^7	1.53	1.54	1.53	1.54	1.54	1.53
N^8-C^9	1.46	1.47	1.47	1.47	1.47	1.49
C^9-C^{10}	1.53	1.53	1.53	1.53	1.53	1.54
C^{10}-C^{11}	1.53	1.54	1.53	1.54	1.54	1.52
C^{11}-N^1	1.47	1.46	1.47	1.46	1.46	1.47
N^1-C^7	1.40	1.44	1.43	1.44	1.44	1.42
N^1-C^2	1.47	1.46	1.47	1.46	1.46	1.47
C^7-N^8	1.29	1.43	1.42	1.43	1.43	1.47

Table 4: Calculated bond angles in degree involving C=N atoms in the optimized DBU and its selected derivatives.

Bond Angles	Compounds					
	DBU	2b	2c	2e	2f	2g
C^2-C^3-C^4	113.22	114.97	114.07	114.70	114.78	114.36
C^3-C^4-C^5	113.43	115.31	113.51	115.17	115.29	114.38
C^4-C^5-C^6	114.26	113.90	114.38	113.89	113.94	114.45
C^5-C^6-C^7	122.27	117.58	116.27	117.71	117.57	115.02
C^6-C^7-N^1	119.13	117.14	112.60	117.27	117.10	115.16
C^6-C^7-N^8	115.04	111.61	115.77	111.61	111.67	117.04
C^7-N^8-C^9	120.79	113.92	116.31	113.91	113.79	113.50
N^8-C^9-C^{10}	114.69	109.62	110.00	109.69	109.66	111.16
C^9-C^{10}-C^{11}	107.45	108.69	109.91	108.71	108.65	109.65
C^{10}-C^{11}-N^1	110.68	109.75	110.15	109.77	109.66	110.26
C^{11}-N^1-C^7	115.61	116.46	115.05	116.59	116.41	115.77
C^{11}-N^1-C^2	118.08	118.40	114.25	118.45	118.58	114.51
N^1-C^7-N^8	125.39	108.75	112.31	108.76	108.74	111.63
N^1-C^2-C^3	114.50	117.76	113.84	117.59	117.68	114.87
C^7-N^1-C^2	119.39	118.73	116.14	118.79	118.80	121.93

2.3.1. HOMO and LUMO energies and band gap

The optimization calculations for the DBU and its derivatives provided HOMO and LUMO energy as well as the band gaps (Table 5). The DBU compound and its derivatives contain both

$\pi-\pi^*$ and $n-\pi^*$ transitions due to the contribution from unsaturated bond and non-bonding electrons. From the molecular orbital calculations, it was assessed that the alkyl substitution at the nitrogen atom made no difference on HOMO and LUMO energies in comparison to the DBU compound, thus leading to an average band gap value of 0.211 except for compounds **2c** and **2g**, whose band gap are 0.215 and 0.218, respectively. The data clearly demonstrate the conjugation effect in these two compounds that leads to enhancement HOMO energy while LUMO energy got reduced. Figure 4 illustrates the visualization of HOMO and LUMO molecular orbitals in compound **2g** in the form of Isosurface.

Table 5: Calculated band gaps for the DBU and its selected derivatives.

Energy	Compounds					
	DBU	**2b**	**2c**	**2e**	**2f**	**2g**
HOMO	-0.21189	-0.21179	-0.21505	-0.21145	-0.21145	-0.22696
LUMO	-0.00269	-0.00035	0.00088	-0.00056	-0.00083	-0.00891
Band Gap	0.20920	0.21144	0.21593	0.21089	0.21062	0.21805

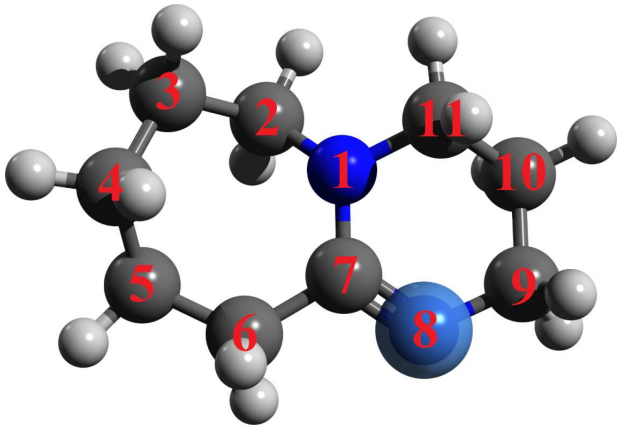

Figure 3: Optimized geometry of the DBU compound **1** with highlighted nitrogen where all substitutions were carried out.

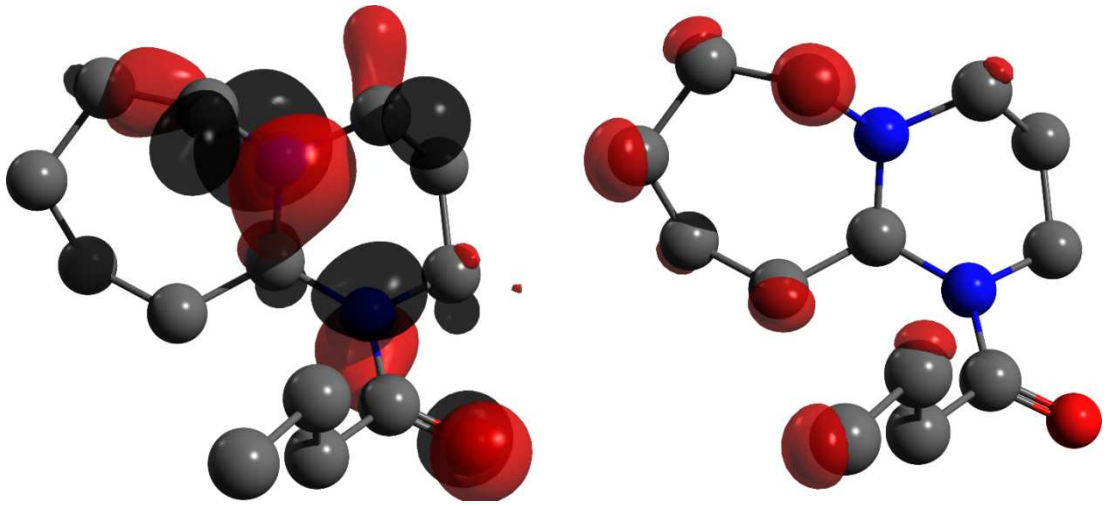

Figure 4: HOMO and LUMO of compound **2g** plotted at isovalue of 0.04.

Stability of DBUF Compounds

The thermal stability of ionic liquids is a unique property that determines its applicability in a number of industrial processes. The relative stabilities of DBU compounds were assessed *via* binding energies obtained from the DFT calculations. The binding energies of the selected DBU compound are listed in Table 6 in comparison to the binding energy value for the TBAF. From the binding energy data, it is obvious that all DBU derivatives have much lower values in the range between -145.15 and -167.65 kcal/mol than that of TBAF compound (-104.25 kcal/mol). Alkyl substituted DBU derivatives have identical binding energies except compound **2c** in which double bond seems to provide intermediate stability to the compound but in case of acyl derivative **2g**, the binding energy value of -167.65 kcal/mol demonstrates a much stable structure compared to other DBU derivatives and TBAF.

Table 6: Calculated binding energies in kcal/mole for selected DBU derivatives in comparison to TBAF.

	Compounds					
	TBAF	**2b**	**2c**	**2e**	**2f**	**2g**
Energy (kcal/mol)	-104.25	-145.15	-154.92	-154.94	-155.40	-167.65

2.4. Solvent-free tetrazole synthesis

For tetrazole synthesis, $TMSN_3$ reagent was used as azide source for coupling with alkyl nitrile in the presence of DBUF-ILs **2a–2j**. Fluoride anion forms a strong bond with its silicon counterpart (Si-F) to release the reactive azide species for [3+2]-cycloaddition in order to get desired tetrazole ring. Tetrazole is a isosteric replacement of carboxylic acid and has significant role in enhancing the efficacy of the bioactive molecules of pharmaceutical interest. The reported methods of tetrazole formation have some disadvantages such as expensive and hygroscopic reagents or toxic metals catalysts along with tedious work up for removal inorganic salts. [23-26] We report a new class of DBU-based ILs **2a-2j**, which have been used as catalyst to perform the click chemistry reaction for tetrazole formation.

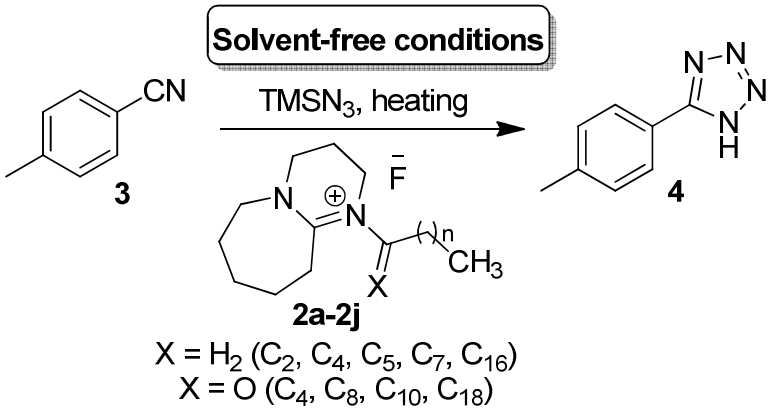

Scheme 2: DBUF-ILs (**2a-2j**) catalyzed tetrazole synthesis

Table 7: Solvent-free tetrazole synthesis under conventional conducting and microwave heating

Compound No.	Reaction Time (h)		Yield (%)	
	Δ[a]	MW[b]	Δ	MW
2a	14	1	40	62
2b	14	0.5	39	70
2c	14	2	21	31
2d	12	1	26	73
2e	12	1	70	75*
2f	12	1	48	80
2g	14	1	20	61

2h	10	1.5	-	80
2i	12	2	-	50
2j	12	1	-	78

[a] = conventional heating (100 °C)
[b] = microwave heating (170 °C)
* Scaled up reaction with 4′-methylbenzonitrile as starting material

An optimal reaction condition of tetrazole formation in solvent-free conditions both under conventional and microwave heating has been established (Table 7). The conversion of starting material **3** to tetrazole **4** was found ~ 50% at 0.5 equiv with a representative ionic liquid **2e**. In case of microwave heating, a slight increase in the yield (55%) was observed. These results predict that 0.5 equiv of IL **2e** deprotect only 50% of *N*-silylated reagents, $TMSN_3$. Excellent yield (80%) of tetrazole was obtained by increasing the equiv of ionic liquid to 1.0 under both heating conditions. Further increase of the IL **2e** equiv (1.5) results in only a slight increase in the yield (90%).The optimized 1.0 equiv of all ILs **2a-2j** were used for the click chemistry of tetrazole formation (Table 6). The click reaction occurred for all DBU based ILs with varying degree of tetrazole yield (31-95%). A scaled-up reaction up to 10 mmol of 4′-methylbenzonitrile **3** was also carried to validate the method at gram scale. As expected, the yield of tetrazole **4** was found lower under conventional conductive heating in comparison to microwave heating.

3. Conclusion:

In summary, we have synthetized a new class of DBU-based fluorinated ILs **2a-2j** *via* quaternization and halides exchanges reactions. The micellization behavior of the DBU derivatives was studied. Size of formed micelles were not affected significantly by the concentration of the ionic liquid, however, there is a clear trend in the hydrodynamic radius with variations in the pH of the solution and temperature treatment. The DFT calculations for geometrical studies have been performed that showed variation in bond lengths and angles of DBU on quaternization. A large HOMO–LUMO energy gap for the compound **2g** demonstrates the conjugation effect of the carbonyl group that is directly attached to unsaturated nitrogen atom. The applicability of DBU-ILs in organic synthesis has been explored. A click reaction of tetrazole formation was under solvent-free condition by using both conventional conductive and

microwave heating modes. Further applications of DBU-ILs in organic synthesis are under investigation.

Material and Methods

DBU (1,8-Diazabicyclo[5.4.0]undec-7-ene, ≥99.0%), alkyl halides, acid halides, potassium fluoride (≥99.0%) were purchased from Sigma Aldrich and used without any purification unless otherwise stated. The HPLC grade methanol (≥99.9%) and distill water were used as solvents. All the reactions include DBU quaternization and tetrazole synthesis under conventional thermal conditions were performed in screw capped Micro Reaction Vessels (3-5 mL), purchased from Sigma Aldrich. For reaction monitoring and column chromatography silica gel 60 aluminium-backed plates having 0.063-0.200 mm as the stationary phase had been used with analytical grad solvents such as methanol, ethyl acetate (EtOAc), diethyl ether, hexane. For TLC spot visualization UV light (254 nm) or using different staining mixtures such as basic potassium permanganate or vanillin had been used. Infrared (IR) spectra and UV spectra were obtained on Bruker Vector-22 spectrometer and Evolution™ 300 UV-Vis Spectrophotometer respectively. The ^{1}H NMR spectra were obtained on Bruker spectrometers at 300 MHz, 400 MHz, 500 MHz, 600 MHz and ^{13}C NMR at 75 MHz, 100 MHz,125 MHz, 150 MHz in the appropriate deuterated solvent. The chemical shifts were recorded on the δ-scale (ppm) using residual solvents as an internal standard (DMSO; ^{1}H 2.50, ^{13}C 39.43 and $CHCl_3$; ^{1}H 7.26, ^{13}C 77.16). Coupling constant were calculated in Hertz (Hz) and multiplicities were labelled s (singlet), d (doublet), t (triplet), q (quartet), quint (quintet) and the prefixes br (broad) or app (apparent) were used. Mass spectra (EI^+ or FAB) were recorded at Finnigan MAT-321A, Germany. Melting points of solids were determined using a Stuart™ melting point apparatus SMP3 apparatus. For micellization studies Dynamic Light Scattering (DLS) Laser Spectroscatter-201 system (RiNA GmbH Berlin, Germany) was used. Analytical HPLC analyses were performed with an Agilent HPLC equipped with a UV-Vis detector. A reverse phase Eclipse Plus C-18 column (4.6 x 100 mm, 3.5µm particle size) with flow rate 0.2 mL/min was used for analytical chromatography. A mixture of HPLC grade acetonitrile and water (6:4) were used as eluents.

Microwave irradiation experimental details: Microwave-assisted synthesis was performed with an Initiator-8 single-mode microwave instrument producing controlled irradiation at 2.450 GHz (Biotage AB, Uppsala), including proprietary Workflow Manager Software (version 2.1).

All the experiments of tetrazole formation were performed in sealed microwave (0.2 to 0.5 mL, 0.5–2.0 mL filling volume) process vials by utilizing the standard absorbance level (400 W maximum power). The reaction time period under microwave conditions refer to hold times at the temperatures indicated, not to total irradiation times. An IR sensor present on outside reaction vessel was used to measure the temperature.

General synthetic procedure of DBUF-ILs (2a-2j)

Step I: An oven dried micro reaction vessels charged with DBU (1 equiv) and corresponding alkyl or acid halides (1.01 equiv.) were mixed together at room temperature and then heated the resulting mixture at 120-125 $^{\circ}$C until no starting material DBU was observed by TLC analysis. The resulting ionic compound was used without purification in the next step.

Step II: In the halides exchanges step, the ionic compound was dissolved in the mixture of solvents (H_2O / MeOH, 1:9 ratio) followed by the addition of potassium fluoride (1.5-3.0 equiv) at room temperature. The resulting mixture was then simply shaked until the complete consumption of starting material, judge by TLC analysis. The crude mixture was then purified by using the silica gel column chromatography with gradient elution by using solvents mixture from EtOAc / Hexane 1:1 to EtOAc / MeOH 9:1.[8] The final ionic compounds with fluoride counter ion **2a-2j** were characterized with ^{1}H, ^{13}C, NMR, IR, UV spectroscopy and mass spectrometry.

Procedure for tetarzole synthesis

An oven dried micro reacting vessel equipped with magnetic bar was flushed with argon. To the vessel DBUF-IL **2a** was added followed by 4′-methyl benzonitrile **3** (1 equiv) and $TMSN_3$ (1.2 equiv) at room temperature. The reaction mixture was then heated at 90-95 $^{\circ}$C until no starting material was observed by TLC analysis. The reaction was then quenched with 1 M HCl (10 mL) and extracted with EtOAc (15 x 3). The combined organic layers was further was washed with 1M HCl (10 mL x 3) to remove the any trace of DBUF-IL. The organic layer was dried with MgSO4, filtered and evaporated *in vacuo* to get the desired the pure 5-(*p*-tolyl)-1*H*-tetrazole **4**, judge by ^{1}H NMR spectrum, as while solid in 31-95% yield with different DBUF-ILs **2a-2j** (Table 6). *Note*: All the reactions were carried out with 1 mmol of 4′-methylbenzonitrile, while a scale up reaction by taking 10 mmol of 4′-methylbenzonitrile (1.17 g) as starting material was also performed under microwave irradiations. The desired tetrazole was obtained in 75% (1.2 g)

yield. ^{1}H NMR (400 MHz, DMSO): δ_H 7.91 (2H, d, J = 8.0 Hz, ArH), 7.39 (2H, d, J = 8.0 Hz, Ar*H*), 2.38 (3H, s, CH_3). The data is identical to those previously reported. [27, 28]

Micellization

Micelles were prepared by direct dissolution of ionic liquids in deionized water. Sample concentrations were varied systematically (0.1 to 7.5 wt. %) to study the effect of concentration on the micellization behavior. Generally, concentration of ionic liquid in the water was kept 1.0 wt.% unless otherwise mentioned. Samples were equilibrated overnight prior to DLS measurements.

Dynamic Light Scattering (DLS) Measurements

DLS studies were performed using a Laser Spectroscatter-201 system (RiNA GmbH Berlin, Germany) with a He-Ne laser providing a 690 nm light source and an output power in the range of 10-50 mW. For all measurements, an autopiloted run of 50 measurements at every 20 sec, with a wait time of 1 sec was used at 30°C. All samples (20 µL), reagents and buffers were filtered using 0.22 µm filter (Millipore, USA) before being introduced into a special quartz SUPRASIL ® cell (light path 1.5 mm) for measurement. The scattered light was collected at a fix scattering angle of 90°. The autocorrelation functions were analyzed with the program CONTIN to obtain hydrodynamic radius (R_H) distributions. The R_H is related to the diffusion coefficient by the Einstein-Stokes equation. The data were analyzed using PMgr v3.01p17 software supplied with the instrument.

For effect of pH on micellization, ionic liquid solution in water (ca. 1 wt. %) is diluted in respective buffer (10x; pH 2 to 12) and keep overnight at room temperature to attain the pH stability before being subjecting to DLS measurements. [29, 30] Temperature stability was checked by heating or cooling the ionic liquid solution at the desired temperature using thermomixer comfort (Eppendorf, Germany) for 15 min. The samples ware then brought to room temperature prior to DLS measurements.

Computational details

A combined approach of synthesis and density functional level studies was adopted to explore structural diversity of the DBU derivatives having different active substituents. Molecular structure of DBU derivatives were built and optimized without any symmetry constraints at DFT

level of theory using B3LYP (Becke, three-parameter, Lee-Yang-Parr) functional and 6-31G + (d) basis sets for all atoms. [31, 32] The optimized structural parameters of these derivatives were obtained from the geometry optimization calculations and were compared with the DBU compound displayed in Figure 3 with highlighted nitrogen atom at which the substitution was carried out. The optimization calculations also enabled to retrieve information of HOMO and LUMO orbital energies and their band gap calculated as difference between the HOMO and LUMO orbital energies. The binding energies for these ionic compounds in comparison to TBAF were also obtained from the optimized geometries. All these calculations were performed employing Gaussian **09**. [33]

Spectral data of Synthetic DBUF-ILs

1-ethyl-2,3,4,6,7,8,9,10-octahydropyrimido[1,2-*a*]azepin-1-ium fluoride (2a) Oily brown solid, 3.75 g (95 %), IR (ν_{max}, cm^{-1}): (Solid, KBr) 3452, 2932, 2863, 1622 (C=N), 1527, 1444, 1388, 1327, 1196. ^{1}H NMR (400 MHz, DMSO): δ_H 3.60 (2H, d, J = 9.2 Hz, CH_2), 3.54 (2H, q, J = 7.2 Hz, CH_2), 3.44 (4H, app quin, J = 5.8 Hz, $(CH_2)_2$), 2.83 (2H, d, J = 10 Hz, CH_2), 1.95 (2H, quin, J = 6.0 Hz, CH_2), 1.68-1.61 (6H, m, $(CH_2)_3$), 1.14 (3H, t, J = 7.2 Hz, CH_3); ^{13}C NMR (100 MHz, DMSO): δ_C 165.6, 53.8, 48.4, 48.1, 45.8, 28.2, 27, 25.4, 22.9, 19.5, 13.6. MS-ESI *m/z* (%), 181 (M^+–F^-, 60), 180 (M^+–H^+–F^- 100); FAB-MS *m/z* 201 (M–H^+).

1-butyl-2,3,4,6,7,8,9,10-octahydropyrimido[1,2-*a*]azepin-1-ium fluoride (2b) Brown oil, 1.33 g (90 %), IR (ν_{max}, cm^{-1}): (Solid, KBr) 3418, 2933, 2862, 1622 (C=N), 1494, 1450, 1373, 1268, 1221, 1112. ^{1}H NMR (400 MHz, DMSO): δ_H 3.61 (2H, d, J = 8.8 Hz, CH_2), 3.50-3.40 (6H, m $(CH_2)_3$), 2.84 (2H, d, J = 10 Hz, CH_2), 1.94 (2H, quin, J = 5.8 Hz, CH_2), 1.70-1.57 (6H, m, $(CH_2)_3$), 1.50 (2H, quin, J = 7.2 Hz, CH_2), 1.94 (2H, sex, J = 7.2 Hz, CH_2), 0.88 (3H, t, J = 7.2 Hz, CH_3); ^{13}C NMR (150 MHz, DMSO): δ_C 165.9, 53.9, 52.9, 48.5, 46.6, 30.3, 27.8, 26.7, 25.5, 22.8, 19.6, 19.2, 13.8. MS-EI *m/z* (%), 228 (M^+, 83), 227 (M–H^+, 27) ; HRMS (M–H^+) $C_{13}H_{24}N_2F$ Found 227.1914, Calculated 227.1923.

***(E)*-1-(but-2-en-1-yl)-2,3,4,6,7,8,9,10-octahydropyrimido[1,2-*a*]azepin-1-ium fluoride (2c)** Brown oil, 1.18 g (80 %), IR (ν_{max}, cm^{-1}): (Solid, KBr) 3416, 2934, 2862, 1621 (C=N), 1527, 1445, 1327, 1197, 1109. ^{1}H NMR (300 MHz, DMSO): δ_H 5.75-5.63 (1H, m, C*H*=CH), 5.49-5.42 (1H, m, CH=C*H*), 4.09 (2H, d, J = 5.1 Hz, CH_2), 3.63-3.60 (2H, m, CH_2), 3.49-3.40 (4H, m,

$(CH_2)_2$), 2.81 (2H, d, *J* = 9.3 Hz, CH_2), 1.96 (2H, quin, *J* = 5.4 Hz, CH_2), 1.69-1.61 (9H, m, $(CH_2)_3$ & CH_3); ^{13}C NMR (100 MHz, DMSO): δ_C 166.1, 128.8, 124.6, 54.4, 54.0, 48.4, 46.5, 27.8, 27.3, 25.5, 22.6, 19.5, 17.5; MS-EI *m/z* (%), 226 (M^+, 3.0), 207 ($M^+–F^–$, 35), 205 (46), 177 (100); FAB-MS *m/z* 227 ($M–H^+$).

1-pentyl-2,3,4,6,7,8,9,10-octahydropyrimido[1,2-*a*]azepin-1-ium fluoride (2d) Brown oil, 3.81 g (80 %), IR (ν_{max}, cm^{-1}): (Solid, KBr) 3446, 2930, 2858, 1623 (C=N), 1492, 1451, 1371, 1199, 1130, 1084. ^1H NMR (400 MHz, DMSO): δ_H 3.61 (2H, d, *J* = 8.8 Hz, CH_2), 3.50-3.38 (6H, m, $(CH_2)_3$), 2.84 (2H, d, *J* = 9.6 Hz, CH_2), 1.95 (2H, quin, *J* = 5.6 Hz, CH_2), 1.70-1.56 (6H, m, $(CH_2)_3$), 1.95 (2H, quin, *J* = 5.6 Hz, CH_2), 1.68-1.58 (6H, m, $(CH_2)_3$), 1.52 (2H, quin, *J* = 7.2 Hz, CH_2), 1.33-1.22 (4H, m, $(CH_2)_3$), 0.86 (3H, t, *J* = 6.8 Hz, CH_3); ^{13}C NMR (125 MHz DMSO): δ_C 165.8, 53.9, 53.1, 48.4, 46.5, 31.1, 28.4, 27.7, 27.1, 25.7, 22.7, 21.9, 19.5, 13.9. MS-ESI 242 ($M–H^+$), 223 ($M^+–F^–$, 100); HRMS ($M–H^+$) $C_{14}H_{26}N_2F$ Found 241.2083, Calculated 241.2080. Analytical HPLC [Sample prepared 5 mg/mL, CH_3CN/Water (6:4), 0.2 mL/min, tR = 4.98 min].

1-heptyl-2,3,4,6,7,8,9,10-octahydropyrimido[1,2-*a*]azepin-1-ium fluoride (2e) Brown oil, 7.84 g (88 %), IR (ν_{max}, cm^{-1}): (Solid, KBr) 3409, 2928, 2857, 1626 (C=N), 1491, 1450, 1372, 1199, 1083. ^1H NMR (400 MHz, DMSO): δ_H 3.60 (2H, d, *J* = 8.4 Hz, CH_2), 3.50-3.40 (6H, m, $(CH_2)_3$), 2.84 (2H, d, *J* = 9.6 Hz, CH_2), 1.94 (2H, quin, *J* = 5.6 Hz, CH_2), 1.70-1.58 (6H, m, $(CH_2)_3$), 1.52 (2H, quin, *J* = 6.4 Hz, CH_2), 1.26 (8H, app brs, $(CH_2)_4$), 0.86 (3H, t, *J* = 6.4 Hz, CH_3); ^{13}C NMR (75 MHz, DMSO): δ_C 165.8, 53.8, 53.0, 48.4, 46.5, 27.8, 27.6, 27.1, 25.4, 22.7, 21.8, 19.5, 13.8. MS-ESI *m/z* (%), 270 (M^+, 54), 269 ($M–H^+$, 100). HRMS (M^+) $C_{16}H_{31}N_2F$ Found 270.2460, Calculated 270.2471. Analytical HPLC [Sample prepared 5 mg/mL, Injection volume 1 μL, CH_3CN/Water (6:4), 0.2 mL/min, tR = 5.14 min].

1-hexadecyl-2,3,4,6,7,8,9,10-octahydropyrimido[1,2-*a*]azepin-1-ium fluoride (2f) Brown oil, 2.06 g (80 %), IR (ν_{max}, cm^{-1}): (Solid, KBr) 3410, 2924, 2853, 1628 (C=N), 1449, 1371, 1201. ^1H NMR (400 MHz, DMSO): δ_H ^1H NMR (400 MHz, DMSO): δ_H 3.60 (2H, d, *J* = 8.8 Hz, CH_2), 3.48-3.40 (6H, m, $(CH_2)_3$), 2.82 (2H, d, *J* = 9.6 Hz, CH_2), 1.88 (2H, quin, *J* = 5.6 Hz, CH_2), 1.70-1.58 (6H, m, $(CH_2)_3$), 1.52 (2H, m, CH_2), 1.23 (26H, app brs, $(CH_2)_{13}$), 0.84(3H, t, *J* = 6.8

Hz, CH_3); ^{13}C NMR (75 MHz, DMSO): δ_C 164.3, 49.0, 46.8, 44.5, 44.2, 31.3, 29.2, 29.0, 28.9, 28.8, 28.7, 28.5 28.3, 25.9, 25.6, 24.5, 23, 22.1, 13.9. MS-ESI *m/z* (%), 395 ($M–H^+$, 100).

1-butyryl-2,3,4,6,7,8,9,10-octahydropyrimido[1,2-a]azepin-1-ium fluoride (2g) Brown oil, 3.33 g (76 %), IR (ν_{max}, cm^{-1}): (Solid, KBr) 3309, 2930, 2861, 1729 (C=O), 1655 (C=N), 1542, 1452, 1369, 1251. ^1H NMR (400 MHz, DMSO): δ_H 3.50 (2H, d, *J* = 8.4 Hz, CH_2), 3.43 (2H, t, *J* = 5.6 Hz, CH_2), 3.22 (2H, t, *J* = 5.6 Hz, CH_2), 2.70 (2H, d, *J* = 10 Hz, CH_2), 1.93-1.84 (4H, m, $(CH_2)_2$), 1.66-1.58 (6H, m, $(CH_2)_3$), 1.42 (2H, sext, *J* = 7.2 Hz, CH_2), 0.81 (3H, t, *J* = 7.6 Hz, CH_3); ^{13}C NMR (100 MHz, DMSO): δ_C 175.2, 163.7, 53.2, 47.8, 41.3, 37.4, 35.6, 31.2, 28.2, 25.9, 23.3, 18.7. FAB-MS *m/z* 241 ($M–H^+$), 223 ($M–F^–$). HRMS ($M–F^–$), $C_{13}H_{23}N_2O$ Found 223.1820, Calculated 223.1810.

1-octanoyl-2,3,4,6,7,8,9,10-octahydropyrimido[1,2-*a*]azepin-1-ium fluoride (2h) Brown oil, 1.50 g (83 %), IR (ν_{max}, cm^{-1}): (Solid, KBr) 2928, 2858, 1718 (C=O), 1644 (C=N), 1449, 1373, 1321, 1212. ^1H NMR (400 MHz, DMSO): δ_H 3.51 (2H, d, *J* = 8.8 Hz, CH_2), 3.44 (2H, t, *J* = 5.6 Hz, CH_2), 3.22 (2H, t, *J* = 5.6 Hz, CH_2), 2.66 (2H, d, *J* = 10 Hz, CH_2), 1.95 (2H, t, *J* = 7.2 Hz, CH_2), 1.88 (2H, quin, *J* = 6.0 Hz, CH_2), 1.70-1.56 (6H, m, $(CH_2)_3$), 1.51-1.49 (2H, m, CH_2), 1.22 (8H, app brs, $(CH_2)_4$), 0.85 (3H, t, *J* = 6.4 Hz, CH_3); ^{13}C NMR (100 MHz, DMSO): δ_C 175.5, 162, 49.0, 45.1, 41.4, 36.4, 35.4, 33.7, 31.2, 29.2, 28.5, 28.4, 25,4, 24.5, 22.1, 13.9. FAB-MS *m/z* 297 ($M–H^+$), 279 ($M–F^–$).

1-dodecanoyl-2,3,4,6,7,8,9,10-octahydropyrimido[1,2-*a*]azepin-1-ium fluoride (2i) Brown oil, 1.61 g (74 %), IR (ν_{max}, cm^{-1}): (Solid, KBr) 2926, 2855, 1743, 1713 (C=O), 1461, 1368, 1170, 1114, 1014. ^1H NMR (400 MHz, DMSO): δ_H 3.52 (2H, d, *J* = 8.8 Hz, CH_2), 3.45 (2H, t, *J* = 5.6 Hz, CH_2), 3.23 (2H, d, *J* = 5.6 Hz, CH_2), 2.66 (2H, d, *J* = 9.6 Hz, CH_2), 2.05 (2H, t, *J* = 7.2 Hz, CH_2), 1.89 (2H, quin, *J* = 5.6 Hz, CH_2), 1.70-1.56 (6H, m, $(CH_2)_3$), 1.45-1.40 (2H, m, CH_2), 1.22 (16H, app brs, $(CH_2)_8$), 0.85 (3H, t, 6.0 Hz, CH_3); ^{13}C NMR (100 MHz, DMSO): δ_C 174.3, 164.2, 51, 33.6, 33.2, 31.3, 28.9, 28.9, 28.8, 28.72, 28.67, 28.64, 28.5, 28.4, 24.5, 24.4, 22.0, 13.8; MS-ESI *m/z* 353 ($M–H^+$), 335 ($M–F^–$).

1-stearoyl-2,3,4,6,7,8,9,10-octahydropyrimido[1,2-*a*]azepin-1-ium fluoride (2j) Brown oil, 2.18 g (80 %), IR (ν_{max}, cm^{-1}): (Solid, KBr) 2925, 2854, 1744 (C=O), 1461, 1363, 1170, 1116. ^1H

NMR (400 MHz, DMSO): δ_H 3.46 (2H, d, J = 8.4 Hz, CH_2), 3.40 (2H, t, J = 5.8 Hz, CH_2), 3.19 (2H, d, J = 5.6 Hz, CH_2), 2.66 (2H, d, J = 10 Hz, CH_2), 2.08 (2H, t, J = 7.2 Hz, CH_2), 1.86 (2H, quin, J = 5.6 Hz, CH_2), 1.69-1.57 (6H, m, $(CH_2)_3$), 1.49-1.45 (2H, m, CH_2), 1.22 (28H, app brs, $(CH_2)_{14}$), 0.85 (3H, t, 6.4 Hz, CH_3); ^{13}C NMR (100 MHz, DMSO): δ_C 175.7, 164.9, 53, 48.5, 48.3, 47.7, 37.7, 36.5, 33.2, 31.2, 31.2, 28.9, 28.6, 28.3, 26.1, 25.9, 23.6, 22.0, 19.2, 13.9; FAB-MS *m/z* 419 ($M–F^-$).

Acknowledgement:

We are thankful to Higher Education Commission (HEC), Pakistan and H. E. J. Research Institute of Chemistry, International Centre for Chemical and Biological Sciences, University of Karachi, Karachi-75270, Pakistan for providing financial support for this project.

Conflict of Interest

The authors have declared no conflict of interest**.**

References:

1. J. P. Hallett and T. Welton, *Chem. Rev.*, 2011, **111**, 3508-3576.
2. P. Wasserscheid and T. Welton, *Ionic Liquids in Synthesis*, Wiley-VCH, Weinheim, Germany, 2008.
3. B. Wu, W. Liu, Y. Zhang and H. Wang, *Chem. Eur. J.*, 2009, **15**, 1804-1810.
4. A.-G. Ying, L.-M. Wang, H.-X. Deng, J.-H. Chen, X.-Z. Chen and W.-D. Ye, *ARKIVOC*, 2009, **xi**, 288-298.
5. X. Chen and A. Ying, in *Ionic Liquids: Applications and Perspectives*, ed. P. A. Kokorin, InTech, 2011.
6. A. Maia, *Mini Rev. Org. Chem.*, 2011, **8**, 178-185.
7. V. K. Aggarwal and A. Mereu, *Chem. Comm.*, 1999, 2311-2312.
8. S. Mahajan, R. Sharma and R. K. Mahajan, *Colloids Surf. A Physicochem. Eng. Asp.*, 2013, **424**, 96-104.
9. B. Yu, H. Zhang, Y. Zhao, S. Chen, J. Xu, L. Hao and Z. Liu, *ACS Catal.*, 2013, **3**, 2076-2082.
10. A.-G. Ying, L. Liu, G.-F. Wu, G. Chen, X.-Z. Chen and W.-D. Ye, *Tetrahedron Lett.*, 2009, **50**, 1653-1657.

11. J. H. Clark, *Chem. Rev.*, 1980, **80**, 429-452.
12. T. Ishikawa, *Superbases for organic synthesis: guanidines, amidines and phosphazenes and related organocatalysts*, Wiley Online Library, 2009.
13. L. V. Myznikov, A. Hrabalek and G. I. Koldobskii, *Chem. Heterocycl. Compd.*, 2007, **43**, 1-9.
14. M. Blesic, M. H. Marques, N. V. Plechkova, K. R. Seddon, L. P. N. Rebelo and A. Lopes, *Green Chem.*, 2007, **9**, 481-490.
15. Z. Miskolczy, K. Sebők-Nagy, L. Biczók and S. Göktürk, *Chem. Phy. Lett.*, 2004, **400**, 296-300.
16. R. Vanyúr, L. Biczók and Z. Miskolczy, *Colloids Surf., A*, 2007, **299**, 256-261.
17. B. Dong, N. Li, L. Zheng, L. Yu and T. Inoue, *Langmuir*, 2007, **23**, 4178-4182.
18. C. Jungnickel, J. Łuczak, J. Ranke, J. F. Fernández, A. Müller and J. Thöming, *Colloids Surf., A*, 2008, **316**, 278-284.
19. T. Inoue, H. Ebina, B. Dong and L. Zheng, *J. Colloid Interface Sci.*, 2007, **314**, 236-241.
20. B. Dong, X. Zhao, L. Zheng, J. Zhang, N. Li and T. Inoue, *Colloids Surf., A*, 2008, **317**, 666-672.
21. O. A. El Seoud, P. A. R. Pires, T. Abdel-Moghny and E. L. Bastos, *J. Colloid Interface Sci.*, 2007, **313**, 296-304.
22. R. Sharma, S. Mahajan and R. K. Mahajan, *Colloids Surf., A*, 2013, **427**, 62-75.
23. J. V. Duncia, M. E. Pierce and J. B. Santella, III., *J. Org. Chem.*, 1991, **56**, 2395-2400.
24. S. J. Wittenberger and B. G. Donner, *J. Org. Chem.*, 1993, **58**, 4139-4141.
25. J. V. Duncia, M. E. Pierce and J. B. Santella, *J. Org. Chem.*, 1991, **56**, 2395-2400.
26. Z. P. Demko and K. B. Sharpless, *J. Org. Chem.*, 2001, **66**, 7945-7950.
27. D.-Y. Hu, X.-W. Chu and Z.-R. Qu, *Acta Crystallogr. Sect. E*, 2009, **65**, o2463.
28. 1995.
29. M. Dulle, M. I. Malik, B. Trathnigg and O. Glatter, *Macromolecules*, 2010, **43**, 7868-7871.
30. A. Iqbal, M. K. Azim, N. Hashmi, S. A. Ali and S. G. Musharraf, *Protein Pept. Lett.*, 2011, **8**, 287-294.
31. K. Kim and K. D. Jordan, *J. Phys. Chem.*, 1994, **98**, 10089-10094.

32. P. J. Stephens, F. J. Devlin, C. F. Chabalowski and M. J. Frisch, *J. Phys. Chem.*, 1994, **98**, 11623-11627.

33. *Gaussian 09, Revision D.01* M. J. Frisch, G. W. Trucks, H. B. Schlegel, G. E. Scuseria, M. A. Robb, J. R. Cheeseman, G. Scalmani, V. Barone, B. Mennucci, G. A. Petersson, H. Nakatsuji, M. Caricato, X. Li, H. P. Hratchian, A. F. Izmaylov, J. Bloino, G. Zheng, J. L. Sonnenberg, M. Hada, M. Ehara, K. Toyota, R. Fukuda, J. Hasegawa, M. Ishida, T. Nakajima, Y. Honda, O. Kitao, H. Nakai, T. Vreven, J. A. Montgomery Jr., J. E. Peralta, F. Ogliaro, M. J. Bearpark, J. Heyd, E. N. Brothers, K. N. Kudin, V. N. Staroverov, R. Kobayashi, J. Normand, K. Raghavachari, A. P. Rendell, J. C. Burant, S. S. Iyengar, J. Tomasi, M. Cossi, N. Rega, N. J. Millam, M. Klene, J. E. Knox, J. B. Cross, V. Bakken, C. Adamo, J. Jaramillo, R. Gomperts, R. E. Stratmann, O. Yazyev, A. J. Austin, R. Cammi, C. Pomelli, J. W. Ochterski, R. L. Martin, K. Morokuma, V. G. Zakrzewski, G. A. Voth, P. Salvador, J. J. Dannenberg, S. Dapprich, A. D. Daniels, Ö. Farkas, J. B. Foresman, J. V. Ortiz, J. Cioslowski and D. J. Fox, 2009